Chemical Physics Letters 633 (2015) 52–57

Contents lists available at ScienceDirect

Chemical Physics Letters

journal homepage: www.elsevier.com/locate/cplett

Field-induced electron localization: Molecular quantum-dot cellular automata and the relevance of Robin–Day classification

Yuhui Lu [a,*], Craig S. Lent [b]

[a] Department of Chemistry, Louisiana College, Pineville, LA 71359, United States
[b] Department of Electrical Engineering, University of Notre Dame, Notre Dame, IN 46556, United States

ARTICLE INFO

Article history:
Received 4 April 2015
In final form 29 April 2015
Available online 11 May 2015

ABSTRACT

Mixed-valence complexes are potential candidates for the molecular quantum-dot cellular automata (QCA) approach, which encodes binary information using the configuration of localized and mobile charges. In the Robin–Day classification of mixed-valence complexes, charge localization/delocalization is determined by the ratio of the nuclear reorganization energy and the electron transfer (ET) matrix element. We point out that the driving force for charge localization in molecular QCA is the Coulomb interaction between neighboring molecules rather than nuclear relaxation. This suggests a different criterion for the relevant charge localization, one based on the ET matrix element and the driving bias of a neighboring molecule.

1. Introduction

Mixed-valence complexes are compounds containing more than one redox center. Mobile electrons can transfer among these redox centers resulting in different charge configurations [1,2]. These compounds are ideal candidates for the study of intramolecular electron and energy transfer [3–5]. Mixed-valence complexes are also potential candidates of molecular electronic devices due to their conductivity and significant nonlinear optical and magnetic properties [6–8]. A large number of mixed-valence complexes have been synthesized and characterized and comprehensive reviews can be found in the literature [9–13].

Our interest in mixed-valence complexes is as a potential molecular implementation of quantum-dot cellular automata (QCA) [14–20], a promising approach to molecular electronics. The key idea in QCA is to encode binary information as the charge configuration of a cell; in this case, the cell is the molecule itself. The simplest QCA cell contains two quantum dots and one mobile charge which can localize on either dot and thereby represent a binary '0' or '1'. Tunneling between the dots enables the device to switch between states. The Coulomb interaction between neighboring cells couples the information from one cell to another, and creates device functionality and information flow. Figure 1a and b schematically illustrates the encoding of binary information in the charge configuration of a two-dot QCA cell and the motion of information in a QCA wire via Coulomb interaction. QCA wires, logic gates, and shift registers, have been demonstrated using small metal islands as dots. More complex circuits, up to the level of microprocessors, have been designed and analyzed [21–23].

The principle advantages of the QCA approach are (1) functional scaling down to the single-molecule limit, and (2) ultra-low power dissipation, so that such scaling is realistic without prohibitive heat generation [24–26]. Metal-island QCA designs are limited to cryogenic operation, but molecular implementations would work at room temperature. A molecular two-dot QCA cell (an architectural half-cell) can be implemented with a mixed-valence compound containing two redox centers. The redox centers act as quantum dots which localize charge, and the tunneling between dots is through the bridge ligands [15].

To be qualified as a QCA candidate molecule, a mixed-valence compound must demonstrate bistability and switchability [27]. Bistability requires that mobile charges should be localized on one or the other of the redox centers. Switchability means that the electric field due to a neighboring cell should be sufficient to switch the molecular state between the bistable configurations.

Localization and delocalization of charge in mixed-valence molecules has long been important in mixed valence chemistry, though the focus has been on the behavior of molecules in solution. In the standard Robin–Day classification scheme [28], charge localization/delocalization in the mixed-valence complexes is determined by the competition between the nuclear reorganization energy λ and the electron transfer (ET) matrix element γ.

* Corresponding author.
E-mail addresses: lu@lacollege.edu (Y. Lu), lent@nd.edu (C.S. Lent).

http://dx.doi.org/10.1016/j.cplett.2015.04.058
0009-2614/

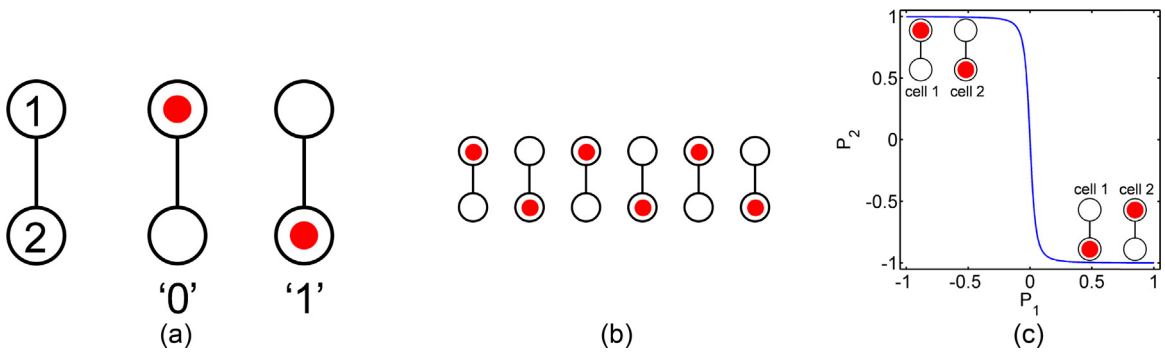

Figure 1. (a) Schematic of a two-dot QCA cell. Binary information is encoded in the charge configuration. (b) A QCA wire. Neighboring cells tend to anti-align due to the Coulomb repulsion. (c) The response function of QCA. One cell's polarization is determined by its neighboring cell's polarization.

Under a two-state approximation [29], the potential energy surfaces for the electron transfer reaction are given by the following equations [10]:

$$E_1 = \frac{[\lambda(2X^2 - 2X + 1)]}{2} - \frac{\{[\lambda(2X-1)]^2 + 4\gamma^2\}^{1/2}}{2} \tag{1a}$$

$$E_2 = \frac{[\lambda(2X^2 - 2X + 1)]}{2} - \frac{\{[\lambda(2X-1)]^2 + 4\gamma^2\}^{1/2}}{2} \tag{1b}$$

Here E_1 and E_2 are the energies of the ground and the first excited states, and X is the reaction coordinate. Based on the relative strength of λ and γ, mixed-valence compounds can be classified as follows:

$$\frac{\lambda}{\gamma} \gg 1, \quad \text{(Class I)}$$

$$\frac{\lambda}{\gamma} > 2, \quad \text{(Class II)}$$

$$\frac{\lambda}{\gamma} < 2, \quad \text{(Class III)}$$

The potential energy surfaces for each class can be found in the literature [10]. Robin–Day classification is a valuable tool for predicting charge localization/delocalization of mixed-valence compounds in solution.

The driving forces for electron transfer solution are the random electric fields imposed on the molecule by its fluctuating environment. The reorganization energy creates a barrier which the driving force must overcome for electron transfer to occur, thus localizing the charge in a stable configuration corresponding a particular nuclear configuration ($X = 0$ or $X = 1$).

QCA, by contrast, uses on a different mechanism for charge localization. QCA depends on Coulomb interaction among neighboring cells in a well-designed device layout to achieve charge localization and bistability [15]. The Coulomb interaction between two neighboring QCA cells is characterized by the cell–cell response function which relates the charge configuration of one cell to the configuration induced in a neighboring cell [14].

For a QCA double-dot molecule, the extent of charge localization and its spatial configuration can be characterized by the cell polarization. The polarization for such a molecule is defined by:

$$P = \frac{\rho_1 - \rho_2}{\rho_1 + \rho_2} \tag{2}$$

where ρ_i is the charge on each charge center i as labeled in Figure 1a. If charge is completely delocalized $P = 0$. Charge completely localized on site 1 (site 2) results in a polarization of +1 (−1). QCA action relies on the polarization of one molecule being Coulombically coupled to the polarization of neighboring molecules. Consider the case of two nearby cells shown in the inset of Figure 1c. For any given polarization of cell 1, labeled P_1, a certain polarization P_2 will be induced in the neighboring cell 2 via Coulomb interactions. The function $P_2(P_1)$, the induced polarization as a function of the neighboring polarization, is the cell–cell response function, shown in Figure 1c.

P_1 and P_2 are quantitatively related through the following expression [27]:

$$P_2 = \frac{2}{1 + \left\{\beta P_1 \sqrt{\beta^2 P_1^2 + 1}\right\}^2} - 1 \tag{3}$$

in which:

$$\beta \equiv \frac{e^2}{4\pi\varepsilon_0}\left(\frac{2-\sqrt{2}}{4}\right)(\gamma L)^{-1} \approx \frac{0.2109\,(\text{eV nm})}{\gamma L} \tag{4}$$

where L is the distance between charge centers in each molecule, here assumed to be arranged so the four centers of two neighboring molecules form a square.

The charge localization and bistability induced by neighboring Coulomb effects can be characterized [27] by the slope of the response function at the origin and the saturated value of $P_2(P_1 - 1)$

$$\left.\frac{dP_2}{dP_1}\right|_{P_{1=0}} = -\beta \tag{5}$$

$$P^{\text{sat}} = \frac{2}{1 + \left(\sqrt{\beta^2 + 1} - \beta\right)^2} - 1 \tag{6}$$

Note that both these measures are determined by the parameter β which is inversely proportional to $\gamma \cdot L$, the product of ET matrix element and the distance between neighboring QCA molecules. The nuclear reorganization energy λ, which plays an important role for Robin–Day classification, is not a determining factor for charge localization of mixed-valence compounds when driven by a neighbor dipole, as in the QCA case. In fact, charge localization due to a neighboring molecule could be effective even if the reorganization energy were zero. On the contrary, if λ is too large, the molecule may become 'stuck' in one polarization and not be switchable by the neighboring molecule.

The motivation of this letter is to demonstrate that for molecular QCA operation, the key is the competition between the driving electric field produced by a neighboring molecule and the ET matrix element—not the competition between the nuclear reorganization energy and the ET matrix element. Therefore Robin–Day classification, though a very useful gauge to classify mixed-valence compounds in solution, is not the decisive factor to determine the qualification of QCA candidate molecules. In particular we want to show quantitatively that class III mixed-valence compounds may be good QCA candidate molecules, exhibiting strong charge localization due to the driving force of the field produced by the neighboring molecule.

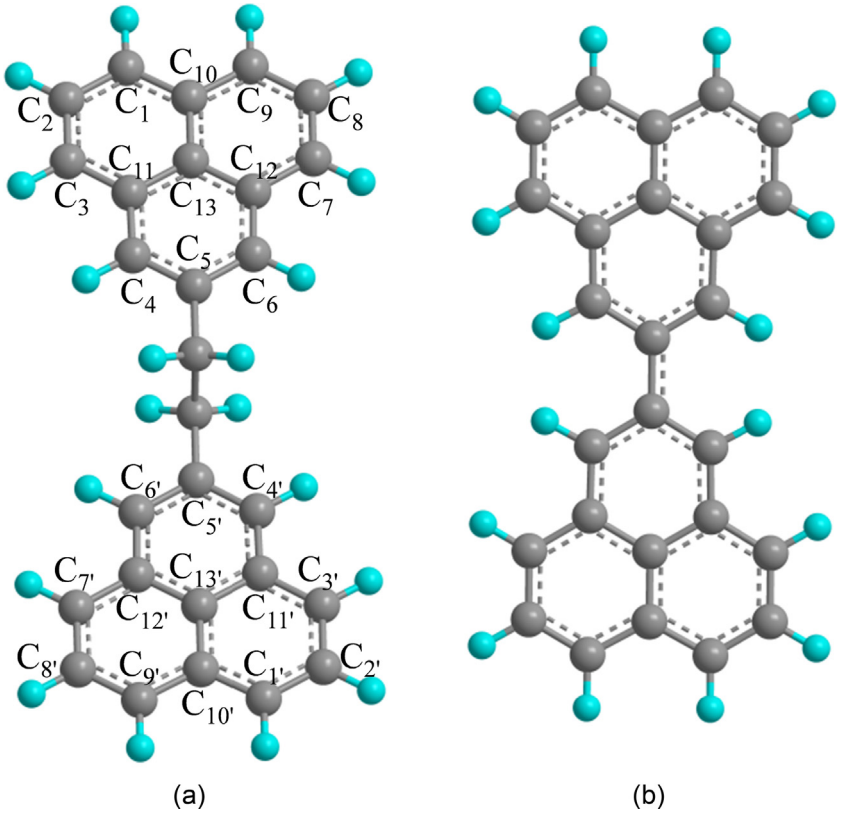

Figure 2. (a) Molecule **1**. 1,2-Diphenalenyl ethane radical cation. (b) Molecule **2**. Biphenalenyl radical cation.

To demonstrate that type III compounds may be suitable QCA molecules, we choose a phenalenyl radical as the building block of QCA candidate molecules, and compute the properties of the model molecules 1,2-diphenalenyl ethane radical cation and biphenalenyl radical cation, hereafter denoted as **1** and **2**, as shown in Figure 2. The phenalenyl radical has gathered attention because of its interesting electric, magnetic, and optical properties [30–32]. We are interested in this moiety due to its small reorganization energy (0.035 eV) [33]. With such small reorganization energy, mixed-valence compounds built from phenalenyl moieties can be Robin–Day class III even if the electronic coupling between redox centers γ is small. As seen by Eqs. (3) and (4), weak electronic communications (small γ) facilitates field-induced charge localization, so charge in these molecules may still be localized by neighboring molecules via Coulomb interaction. The computation of **1** and **2** include geometry optimizations, potential energy surfaces, and the QCA response function. All computations have been conducted using the GAUSSIAN 09 software package [34] at the state average (with weighting coefficients of 0.5 for both the ground and first excited states) complete active space self-consistent field CASSCF(1,2) level [35,36] with 6-31G* basis set for all atoms.

Molecule **1** has two stable charge configurations. Figure 3 shows the highest occupied molecular orbitals (HOMO) and the

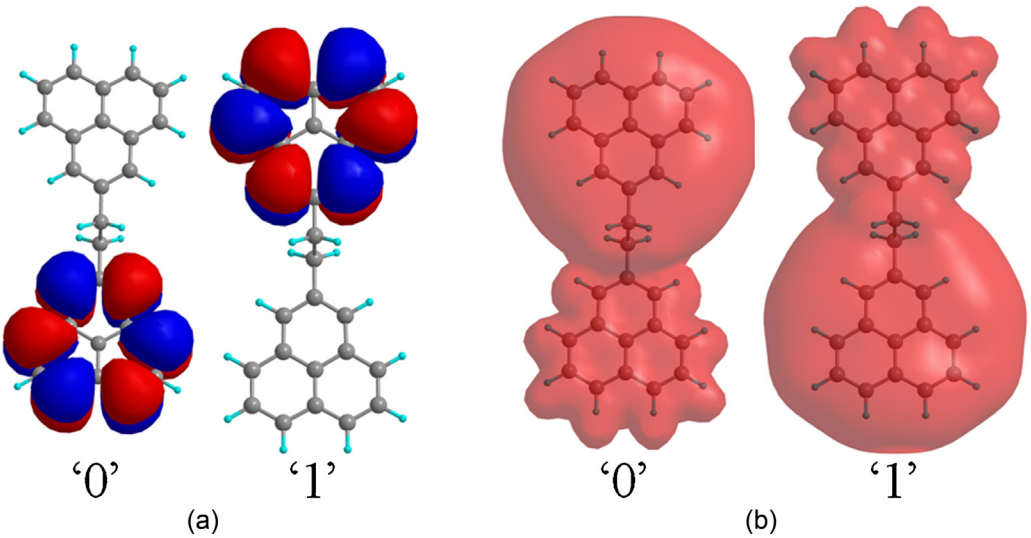

Figure 3. Bistable charge configuration of molecule **1**, 1,2-Diphenalenyl ethane radical cation. The bistability is shown by (a) HOMO orbitals, and (b) the electrostatic isopotential surface. Either phenalenyl group can be positively charged. The different charge configurations are used to represent '0' and '1' state.

Table 1
The optimized structural parameters (in Å) of molecule **1**. Atoms are numbered as shown in Figure 2.

	C_2—C_3	C_3—C_{11}	C_{10}—C_{13}	C_{11}—C_{13}	$C_{2'}$—$C_{3'}$	$C_{3'}$—$C_{11'}$	$C_{10'}$—$C_{13'}$	$C_{11'}$—$C_{13'}$
'0'	1.384	1.408	1.410	1.408	1.379	1.412	1.421	1.418
'1'	1.379	1.412	1.421	1.418	1.384	1.408	1.410	1.408

electrostatic isopotential surface. For **1**, the HOMO is a singly occupied molecular orbital (SOMO), which has a strong nonbonding character [33]. The unpaired mobile electron can localize on either phenalenyl groups resulting in bistable configurations suitable for encoding binary information '0' and '1'. The Mulliken charge distribution analysis shows that for the '0' state, the charge density of the upper phenalenyl group is about +1; and for the '1' state, one unit positive charge is localized on the lower phenalenyl group. The optimized geometries of both '0' and '1' states are given in Table 1. The most conspicuous differences between the neutral and cationic phenalenyl moities are bondlength between C_{10}—C_{13} and C_{11}—C_{13} (atoms are numbered in Figure 2). Compared to the cationic phenalenyl, those bonds are 0.1 Å longer when the phenalenyl is neutral. This geometrical difference is reasonable because of the nonbonding character of the SOMO, the occupation of which tends to strengthen electron repulsion hence elongating bond length.

Figure 4a shows potential energy surfaces of the ground state and the first excited state of molecule **1**. The reaction coordinate is determined by linearly combining the nuclear geometries of the '0' and '1' states. The results from CASSCF computation and the two-state approximation, as calculated using Eq. (1), are clearly in good agreement. Our computation shows the reorganization energy and the ET matrix element of **1** are $\lambda = 0.05$ eV and $\gamma = 0.003$ eV, respectively. According to the Robin–Day classification, **1** is a class II mixed-valence compound, which means the nuclear relaxation is sufficient to localize the mobile electron on either phenalenyl moiety. This is consistent with Figure 3, which demonstrates the bistable charge configuration due to the nuclear geometry optimization. Figure 4b shows the polarization as a function of the reaction coordinate, from which one can see the polarization responds nonlinearly to the reaction coordinate. The molecule is fully polarized at $X = 0$ and $X = 1$. At the transition state where $X = 0.5$, the molecule is completely depolarized: the mobile electron is evenly delocalized between two phenalenyl sites. Figure 4a and b are closely related: for class II mixed valence compound, the effect of nuclear relaxation overcomes the communication (tunneling) between the donor and acceptor, therefore the mobile charge can be localized by the nuclear relaxation.

From the perspective of QCA implementations, the bistability of **1** can also be induced by the Coulomb repulsion between neighboring molecules. To explore the effect of neighboring Coulomb repulsion on **1**, we compute the energy and charge distribution

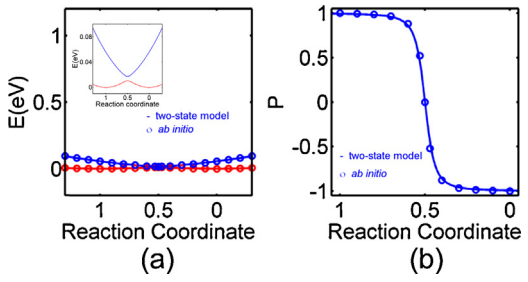

Figure 4. The effects of nuclear relaxation on the energy and charge distribution of molecule **1**, 1,2-diphenalenyl ethane radical cation. (a) Potential energy surfaces of the ground and excited states. The inset, which presents the same potential energy surfaces at a different scale, demonstrates two local minimum on the ground state. (b) Polarization of **1** as a function of the reaction coordinate.

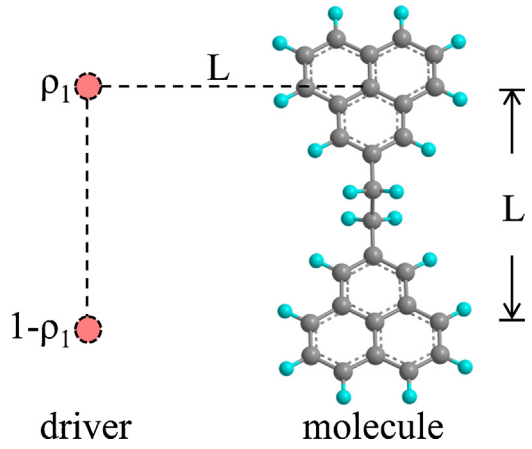

Figure 5. Coulomb interaction between two neighboring molecules. A driver molecule is mimicked by two point charges. The charge density of each point varies from 0 to 1. The distance between the driver and the target molecule, set the same as the phenalenyl–phenalenyl distance in **1**, is 9.4 Å.

of **1** as functions of a neighboring driver molecule's polarization. The driver employed here consists two positive point charges apart away from each other at a separation of 9.4 Å, the same as the phenalenyl–phenalenyl distance of **1**. The charge density of the two points can vary but the total charge density of the driver is maintained as +1 to mimic a neighboring molecular cation. The distance between the driver and the target molecule is also set to be 9.4 Å, such that four charge centers form a square as shown in Figure 5.

Figure 6a shows the calculated energies of the ground and first excited states at the transition state geometry ($X = 0.5$) as functions of the polarization of a neighboring molecule, mimicked by the two-point driver (Figure 5). When the driver's polarization is zero—corresponding to the configuration the driver charge is completely delocalized, the energy gap between the ground and first excited state is 2γ. That gap increases nearly linearly as the driver's polarization increases. When the driver is fully polarized, the gap between the two lowest energy levels is about 0.4 eV. This 'kink energy' defined by

$$E_k = (E_2 - E_1)\big|_{P_1=1} = (E_2 - E_1)\big|_{P_1=-1}$$

is the energy difference between the 'correct' and 'wrong' charge configurations when the driver is completely polarized, and represent the maximum driving bias that a neighboring molecule

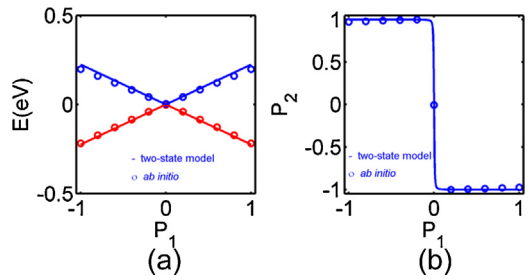

Figure 6. Switching of molecule **1** induced by a point charge driver. (a) Energy diagram. (b) Cell–cell response function. The results shown are obtained from the state average CASSCF method (dots) and the two-state model (solid line).

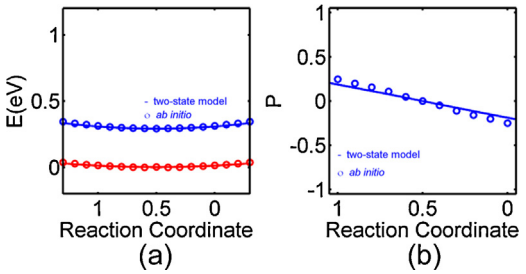

Figure 7. The effects of nuclear relaxation on the energy and charge distribution of molecule **2**, biphenalenyl radical cation. (a) Potential energy surfaces of the ground and excited states. (b) Polarization of **2** as a function of reaction coordinates.

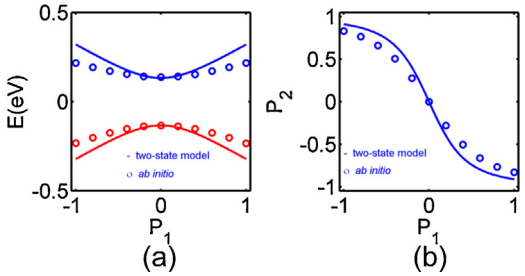

Figure 8. Switching of molecule **2** induced by a point charge driver. (a) Energy diagram. (b) Cell–cell response function. The results shown are obtained from the state average CASSCF method (dots) and the two-state model (solid line).

can provide to localize mobile electron in QCA molecules. The kink energy is uniquely determined by the intra-dot-dot distance and inter-cell–cell distance, but independent of the reorganization energy.

For molecule **1**, the communication between the two redox centers is rather weak ($\gamma = 0.003$ eV), therefore it can be fully polarized by a driver according to Eqs. (3) and (4). This strong bistability is shown by the cell–cell response function in Figure 6b, which presents the computed polarization (equivalent to a scaled dipole moment) of the ground state as a function of the driver's polarization. It can be seen from Figure 6b that the driver can induce an opposite dipole moment in its neighboring molecule. Since the computation is conducted at $X = 0.5$ this demonstrates that even without nuclear relaxation, the Coulomb interaction alone is sufficient to localize the mobile charge of the neighboring molecules and binary information can be transported in QCA arrays via Coulomb interaction, thus satisfying two basic requirements for QCA operation.

Figures 4 and 6 demonstrate that the mobile charge in molecule **1** can be localized by two mechanisms: nuclear relaxation and neighboring Coulomb repulsion. Nuclear relaxation can cause charge localization because **1** is a class II mixed-valence compound so nuclear relaxation can overcome the communication between two redox centers. The Coulomb repulsion between neighboring molecules is capable of localizing the mobile electron because the ET matrix element is small, compared to the driving bias. It is notable that for both localization by nuclear relaxation and localization by Coulomb interaction, the ab initio state average CASSCF computations are in good agreement with the two-state approximation.

For molecule **2**, we also computed the energy levels and the charge distribution as functions of the reaction coordinate. Figure 7a presents energies of the two lowest lying levels. Unlike molecule **1**, there is only one minimum on the ground state potential energy surface, which corresponds to the symmetric geometry where $X = 0.5$. We optimized the nuclear geometry with various initial geometric parameters, and all these efforts failed to localize the mobile electron to one phenalenyl group or the other. To construct the reaction coordinate of **2**, we define $X = 0$ and $X = 1$ by using the phenalenyl geometric parameters of molecule **1**, and linearly combine these two geometries for all other values of X. Using the reaction coordinate so defined, our computation shows the nuclear reorganization energy and ET matrix element are 0.05 eV and 0.14 eV, respectively. The ET matrix element of **2** is significantly higher than that of the **1**, because the ET matrix element decreases exponentially with the distance between the two redox centers [27]. According to the Robin–Day classification, **2** is a class III mixed-valence compound. This explains why bistable configurations cannot be obtained through nuclear relaxation and thus only one minimum is found on the ground state potential energy surface. As a class III compound, the nuclear relaxation effect is not sufficient to overcome the communication between two redox centers therefore the mobile electron always delocalizes over the donor and acceptor. The polarization of molecule **2** against the reaction coordinate is plotted in Figure 7b. One can see the charge distribution responds linearly to the reaction coordinate. Even at $X = 0$ or $X = 1$, the polarization is less than 0.3.

However, Figure 8 demonstrates the switching behavior of molecule **2** under the effect of a neighboring driver molecule, mimicked by the two-charge driver. When the driver is depolarized—the mobile charge is evenly distributed over two sites ($P_1 = 0$), the energy difference between the ground and first excited states for the target molecule is 0.28 eV (2γ). The energy gap enlarges as the polarization of the driver increases. The kink energy $E_k = 0.5$ eV. The cell–cell response function of **2** is given in Figure 8b. One can see the response function demonstrates strong nonlinearity. The saturation polarization is more than 0.8 when the driver is fully polarized. Comparing Figures 7b and 8b it can be seen that for molecule **2**, a class III compound, the nuclear reorganization energy is not sufficient to overcome communication between two redox centers and thus the mobile charge is delocalized. But, importantly, the mobile charge *can* be localized by the presence of a nearby driver molecule; the Coulomb repulsion exerted by the neighboring molecule (of the same type) is strong enough to overcome the communication between redox centers and create charge localization. The criteria for relevant QCA localization and switchability are simply:

$$\frac{\gamma}{E_k} \ll 1, \qquad \text{and}$$

$$\frac{\gamma}{E_k} \ll 1.$$

The first requirement needs to be satisfied so the driving force (E_k) is sufficient to overcome the charge delocalization due to the communication between redox centers, and the second condition is to guarantee the mobile change not being trapped by the nuclear relaxation. We recognize nuclear relaxation does play a role in QCA operation, though that effect is secondary. More detailed discussion on nuclear effects, particularly of Robin–Day type I mixed-valence compounds, will be addressed in future studies.

In summary, QCA uses Coulomb interaction, not nuclear relaxation, to create charge localization and switchable bistability which is potentially useful for encoding binary information. We have examined two model mixed-valence compounds, 1,2-diphenalenyl ethane radical cation, molecule **1**, and biphenalenyl radical cation, molecule **2**, using the state-of-the-art CASSCF method. As a class II compound with small ET matrix element, **1** can demonstrate charge localization via both mechanisms: nuclear relaxation and inter-molecular Coulomb repulsion. For molecule **2**, a class III compound, bistability cannot be generated via nuclear relaxation. Yet as a mixed-valence compound with weak donor–acceptor communication, the mobile charge can be localized if a driver is present nearby. Therefore molecule **2**, though a class III mixed-valence

compound according to the Robin–Day classification, may still be used as a QCA candidate molecule (at least as far as the bistability and switchability requirements are concerned). Our conclusion is that, the Robin–Day classification is not the determining factor for screening QCA candidate molecules. The key to QCA functionality is the localization due to the real-space barrier between dots and the symmetry-breaking electric field from a neighboring molecule. The electrostatic interaction provides a strong and dynamic bias which controls the direction of localization from one dot to the other. In QCA, electron transfer is not caused by random thermal motion of nuclei, but by the intentional switching of an operating device.

Acknowledgements

This work was funded by the National Science Foundation through the grant CHE-1124762 and by the Louisiana Board of Regents through the grant NSF(2013)-LINK-78.

References

[1] C. Creutz, H. Taube, J. Am. Chem. Soc. 91 (1969) 3988.
[2] C. Creutz, H. Taube, J. Am. Chem. Soc. 95 (1973) 1086.
[3] N.S. Hush, Coord. Chem. Rev. 64 (1985) 135.
[4] N.S. Hush, A.T. Wong, G.B. Bacskay, J.R. Reimers, J. Am. Chem. Soc. 112 (1990) 4192.
[5] J.C. Curtis, J.S. Bernstein, R.H. Schmehl, T.J. Meyer, Chem. Phys. Lett. 81 (1981) 48.
[6] A. Aviram, J. Am. Chem. Soc. 110 (1988) 5687.
[7] S. Fraysse, C. Coudret, J.-P. Launay, Eur. J. Inorg. Chem. (2000) 1581.
[8] D. Astruc, Acc. Chem. Res. 30 (1997) 383.
[9] R.J. Crutchley, Adv. Inorg. Chem. 41 (1994) 273.
[10] K.D. Demadis, C.M. Hartshorn, T.J. Meyer, Chem. Rev. 101 (2001) 2655.
[11] A. Ceccon, S. Santi, L. Orian, A. Bisello, Coord. Chem. Rev. 248 (2004) 683.
[12] J. Hankache, O.S. Wenger, Chem. Rev. 111 (2011) 5138.
[13] B.S. Brunschwiq, C. Creutz, N. Sutin, Chem. Soc. Rev. 31 (2002) 168.
[14] C.S. Lent, P.D. Tougaw, W. Porod, G.H. Bernstein, Nanotechnology 4 (1993) 49.
[15] C.S. Lent, B. Isaksen, M. Lieberman, J. Am. Chem. Soc. 125 (2003) 1056.
[16] Y. Lu, R. Quardokus, C.S. Lent, F. Justaud, C. Lapinte, S.A. Kandel, J. Am. Chem. Soc. 132 (2010) 13519.
[17] Y. Lu, C.S. Lent, Phys. Chem. Chem. Phys. 13 (2011) 14928.
[18] R. Quardokus, Y. Lu, N.A. Wasio, C.S. Lent, F. Justaud, C. Lapinte, S.A. Kandel, J. Am. Chem. Soc. 134 (2012) 1710.
[19] N.A. Wasio, R.C. Quardokus, R.P. Forrest, S.A. Corcelli, Y. Lu, C.S. Lent, F. Justaud, C. Lapinte, S.A. Kandel, J. Phys. Chem. C 116 (2012) 25486.
[20] Y. Lu, C.S. Lent, Chem. Phys. Lett. 582 (2013) 86.
[21] I. Amlani, A.O. Orlov, G. Toth, G.H. Bernstein, C.S. Lent, G.L. Snider, Science 284 (1999) 289.
[22] A.O. Orlov, I. Amlani, G. Toth, C.S. Lent, G.H. Bernstein, G.L. Snider, Appl. Phys. Lett. 74 (1999) 2875.
[23] K.K. Yadavalli, A. Orlov, J.P. Timler, C.S. Lent, G.L. Snider, Nanotechnology 18 (2007) 375401.
[24] J. Timler, C.S. Lent, J. Appl. Phys. 91 (2002) 823.
[25] C.S. Lent, M. Liu, Y. Lu, Nanotechnology 17 (2006) 4240.
[26] Y. Lu, M. Liu, C.S. Lent, J. Appl. Phys. 102 (2007) 034311.
[27] Y. Lu, C.S. Lent, Nanotechnology 19 (2008) 155703.
[28] M.B. Robin, P. Day, Adv. Inorg. Chem. Radiochem. 10 (1968) 247.
[29] M.D. Newton, Chem. Rev. 91 (1991) 767.
[30] T. Taniguchi, T. Kawakami, K. Yamaguchi, Polyhedron 24 (2005) 2274.
[31] J. Huang, M. Kertesz, J. Phys. Chem. A 111 (2007) 6304.
[32] B. Kolb, M. Kertesz, T. Thonhauser, J. Phys. Chem. A 117 (2013) 3642.
[33] Y.-C. Chang, I. Chao, J. Phys. Chem. Lett. 1 (2010) 116.
[34] M.J. Frisch, et al., Gaussian 09, Revision D.01, Gaussian, Inc., Wallingford, CT, 2009.
[35] M.J. Frisch, I.N. Ragazos, M.A. Robb, H.B. Schlegel, Chem. Phys. Lett. 189 (1992) 524.
[36] N. Yamamoto, T. Vreven, M.A. Robb, M.J. Frisch, H.B. Schlegel, Chem. Phys. Lett. 250 (1996) 373.